Remote Sensing Applications: Society and Environment 17 (2020) 100274

Contents lists available at ScienceDirect

Remote Sensing Applications: Society and Environment

journal homepage: http://www.elsevier.com/locate/rsase

Channel stability assessment in the lower reaches of the Krishna River (India) using multi-temporal satellite data during 1973–2015

Jobin Thomas [a], Sachidanand Kumar [a,b], K.P. Sudheer [a,c,*]

[a] Department of Civil Engineering, Indian Institute of Technology Madras, Chennai, 600 036, India
[b] Department of Civil Engineering, Indian Institute of Technology (Indian School of Mines), Dhanbad, 826 004, India
[c] Department of Agricultural and Biological Engineering, Purdue University, West Lafayette, IN, 47907, USA

ARTICLE INFO

Keywords:
Bank erosion
Remote sensing
Floods
Nagarjuna Sagar Dam
Krishna River

ABSTRACT

The present study examines the extent of erosion and deposition along the banks of the lower reaches of the Krishna River (India) between 1973 and 2015, by analyzing the shifts in the bank lines using Landsat images of the years 1973, 1991 and 2015. The analysis is limited to the river segment downstream of the Nagarjuna Sagar Dam up to the Krishna Delta (318 km). The results indicated that the total area lost between 1973 and 1991 due to bank erosion was 3093 ha, whereas the areal extent was reduced to 1386 ha during 1991–2015. Although the individual river reaches had characteristic bank shifting patterns during the period, most of the reaches shifted their banks without changing the bankfull width of the river. Bank erosion was dominated in most of the study reaches during 1973–1991, compared to deposition, while the pattern was reversed during 1991–2015. The contrasting bank erosion/deposition patterns between 1973-1991 and 1991–2015 might be the reflection of the variations in the pattern of flood events between the periods. The impact of the Nagarjuna Sagar Dam on bank erosion is apparent as a sharp increase in the erosion intensity downstream of the dam. The spatial variability of bank erosion is also a function of regional lithology, with marked variability between the Quaternary sediments and other lithological types.

1. Introduction

Alluvial rivers are highly dynamic landforms, where channel geometry and river morphology are exceptionally sensitive to water discharge, sediment load and active tectonics (Leopold et al., 1964; Ouchi, 1985; Schumm et al., 2000). Alluvial channels are formed by a river in its own sediments, which it has transported and deposited during the present hydrologic regime, and are associated with an older sediment complex at depth (Schumm, 2005; Church, 2006). The key drivers of modification of alluvial river morphology include various natural and anthropogenic factors, such as climate change, alteration of land use/land cover, urbanization, construction of hydraulic structures and flow regulation, river stabilization measures and extraction of fluvial sediments (Surian, 1999; Rinaldi, 2003; Gregory, 2006; Lane et al., 2007; Korhonen and Kuusisto, 2010; Comiti et al., 2011; Radoane et al., 2013; Abate et al., 2015; Morais et al., 2016; Joshi and Jun 2018). Adjustments in channel geometry and morphology (due to bank erosion and deposition, downcutting, degradation and aggradation of bed) reflect an important mechanism of channel response and energy dissipation in alluvial river channels (Simon et al., 2000; Yao et al., 2011). Bank erosion is considered to be a geomorphic process in the perspective of long-term geomorphic evolution of fluvial systems and is integral to the functioning of river ecosystems (Piegay et al., 1997, 2005; Florsheim et al., 2008). On the other hand, bank erosion has many adverse effects on the land and water resources, which qualifies it as a natural hazard to be managed. The socio-economic and environmental issues related to bank erosion of alluvial rivers, causing human vulnerability (e.g., dislocation and resettlement, loss of agricultural land and livelihood, etc.) are a matter of grave concern in the context of sustainable river basin management (Mutton and Haque, 2004; Das, 2011).

In general, bank erosion of alluvial channels is promoted by three different, but interrelated processes, such as subaerial weakening and weathering, mass wasting (including various types of slides and slab failures) and fluvial entrainment (Thorne, 1982; ASCE, 1998; Couper and Maddock, 2001). The extent and nature of bank erosion depend on the force exerted on the bank material by streamflow vis-à-vis the bank resistance (Knighton, 1984). River systems exhibit enormous variability in channel characteristics due to the heterogeneity in the fluvial and

* Corresponding author. Department of Civil Engineering, Indian Institute of Technology Madras, Chennai, 600 036, India.
E-mail address: sudheer@iitm.ac.in (K.P. Sudheer).

https://doi.org/10.1016/j.rsase.2019.100274
Received 5 March 2019; Received in revised form 19 August 2019; Accepted 27 October 2019
Available online 31 October 2019

mass wasting processes operating at a wide range of spatial and temporal scales, resulting in highly variable rates of bank erosion and deposition, and thereby complex patterns of planform evolution. Hence, systematic and periodic assessment of changes in channel characteristics helps identify the issues associated with channel instability caused by bank erosion. Understanding the nature, rates, and causes of the changes in channel geometry and morphology has vital importance to river corridor management and hazard zoning (Gilvear, 1999). Further, spatio-temporal assessment of the changes in channel morphology facilitates improved understanding of the sensitivity of alluvial channels to the changes in the natural and anthropogenic drivers, and thus serves as a guidance for management of large alluvial river systems (Surian and Rinaldi, 2003; Brierley et al., 2008; Downs et al., 2013).

Large alluvial rivers of India were subjected to a long history of anthropogenic modifications, particularly during the post-independence period of Indian history, due to intensification of agriculture, construction of multi-purpose dams and reservoirs, changes in land use/land cover types of riparian belts, floodplains and upstream catchments, modification of topography, industrial development and rapid urbanization, which together led to degradation of the river systems (Smakhtin and Anputhas, 2009). Long-term changes in channel morphology of the large alluvial river systems of India were analyzed by numerous researchers using current and historical remote sensing data. However, such change detection studies were mostly carried out in the Ganges-Brahmaputra River System (e.g., Goswami et al., 1999; Jain and Sinha, 2004; Sarma, 2005; Sarma et al., 2007; Takagi, 2007; Sarkar, 2012; Sarma and Acharjee, 2012; Dewan et al., 2017; Mukherjee et al., 2017), and the river systems of the Indian Peninsula remained unaddressed (Sudhakar and Sudhakar, 2019) until the implementation of the 'R&D Programme in Water Sector' in the Twelfth Five Year Plan (2012–17) of Government of India, for comprehensive river morphological studies to understand the behaviour of the major river systems of India and to evolve effective strategies to overcome the problems through implementation of river management strategies (MoWR, 2016).

Among the different river basins of the Indian Peninsular region, Krishna River Basin (KRB) is typical while considering the basin closure as a result of the rapid expansion of irrigated agriculture (Biggs et al., 2007). The hydrologic regime of the river system underwent severe modification, during the pre-independence period itself, due to the agricultural development coupled with the construction of major and minor irrigation schemes and water diversion structures (Venot et al., 2011). Among the 30 river basins characterized as global level priorities for the protection of aquatic biodiversity, the KRB is one among the nine river basins from India and categorized as "strongly affected" by flow fragmentation and regulation (Groombridge and Jenkins, 1998; Nilsson et al., 2005). Hence, this study examines the extent of bank erosion and deposition of the lower reaches (i.e., downstream of the Nagarjuna Sagar Dam) of the KRB. Specific objectives of the study are: (i) to quantify the areal extent of bank erosion and deposition between 1973 and 2015 and (ii) to identify the drivers responsible for the river channel changes. It is expected that the assessment of bank erosion and deposition may serve as a background reference for developing comprehensive river management strategies and restoration measures for the degraded river system.

2. Study area

The KRB is the fourth largest drainage system of India (in terms of both drainage area and discharge) following the rivers systems, viz., Ganges-Brahmaputra, Indus and Godavari. The Krishna River originates in the Western Ghats and debouches into the Bay of Bengal. The

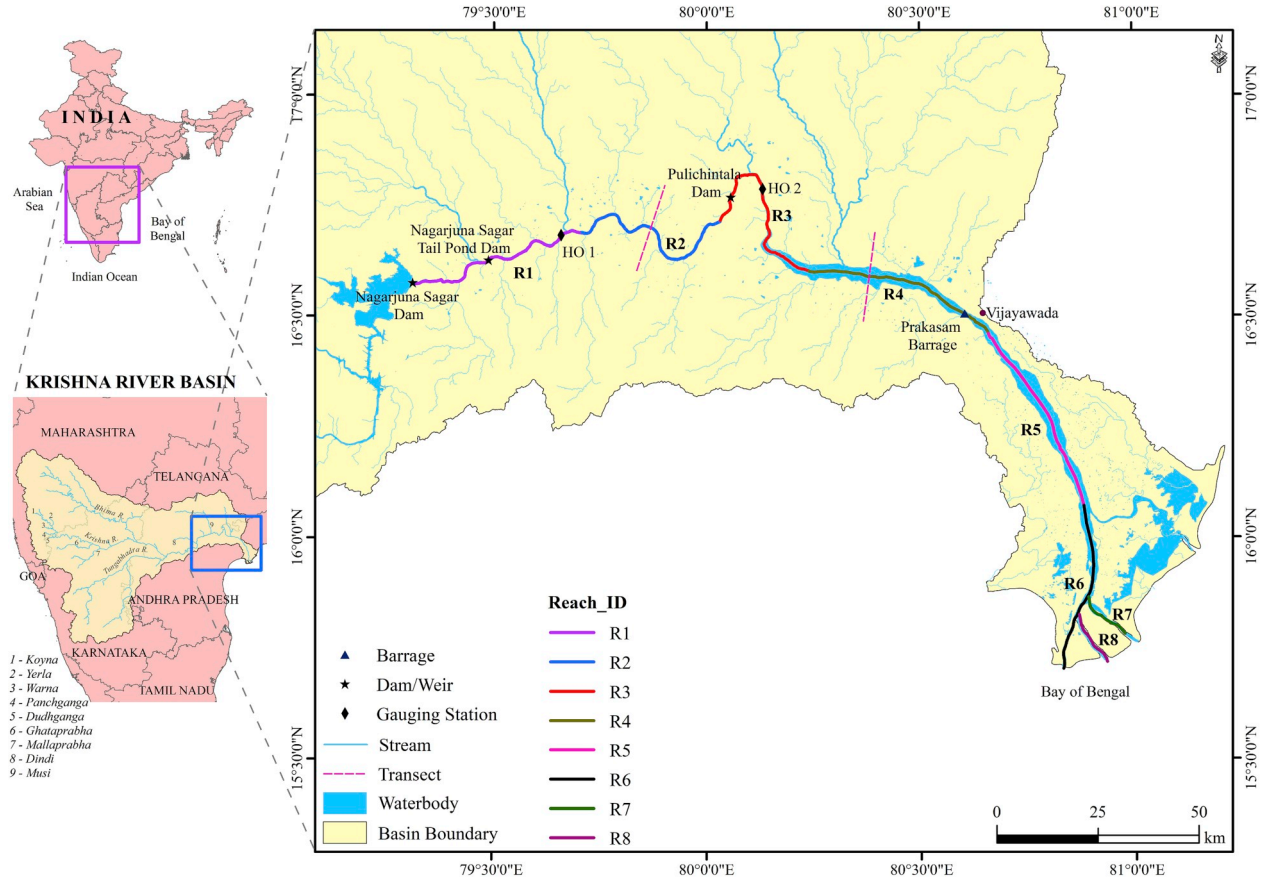

Fig. 1. Location map of the study reaches (R1 to R8) in the Krishna River, India.

catchment area of the basin (2,58,948 km^2) extends between N Lat. 13° 05′ 58″ and 19° 24′ 36″ and E. Long. 73° 20′ 28″ and 81° 12' 42" (Fig. 1). Approximately 44% area of the basin belongs to Karnataka State, 27% to Maharashtra State and 29% to both Telangana and Andhra Pradesh States. Even though several tributaries, such as Koyna, Yerla, Warna, Panchganga, Dudhganga, Ghataprabha, Mallaprabha, Bhima, Tungabhadra, Dindi and Musi feed the Krishna River, the Bhima River from the northwest and the Tungabhadra River from the west to southwest are the two major tributaries. The mainstream length of the river is about 1400 km. However, the present study is restricted to the lower reaches of the river, i.e., downstream of the Nagarjuna Sagar Dam to the Krishna Delta (Fig. 1). The total length of the river segment is 318 km, which was segmented into eight reaches (Table 1) to evaluate the spatial variability in bank erosion and deposition.

The drainage network of the basin is developed on a wide spectrum of geological formations of the Indian Peninsula, ranging in age from the Precambrian to Recent, which include granitoid and metasediments (Achaean to Proterozoic), the sedimentaries (Mesoproterozoic to Neoproterozoic), the Deccan traps (Upper Cretaceous to Paleogene), and fluvial, fluvio-marine, aeolian and coastal sediments (Quaternary). The study reaches downstream of the dam (R1 to R4) have been developed in the lithological types, viz., charnockite, peninsular gneisses, migmatites, (Srisailam) quartzite, and the rocks of Kurnool Group (e.g., coarse-grained sandstone, limestone and quartzite) and Cumbum Formation (e.g., banded slate, graded rhythmite, quartzite and dolomite) (Fig. 2). However, lower parts of R4 as well as the reaches, R5 to R8 have been developed in the Quaternary sediments.

Even though the maximum elevation of the basin is around 1910 m above mean sea level, roughly 90% of the basin area lies below 750 m above mean sea level. Fluvially-dissected hilly terrain (in the western portion) and the Deccan plateau (in the northwestern parts) characterize the upstream portion of the basin, whereas downstream areas have gently undulating topography with wide valleys. Irrespective of the physiography and lithological types, the mainstream of the KRB manifests incised meandering sections at several places (e.g., upstream of Nagarjuna Sagar reservoir). In general, the reaches R1 to R3 are developed in fairly broad valleys covered with unconsolidated sediments. However, the deep river courses developed in such a valley setting imply the stability of the river channels. Braided channels are developed between the reaches R4 and R6 (Fig. 3), where the bars are composed dominantly of coarse to fine sand fractions. The Krishna Delta, occurring in the downstream of the basin, is comprised of sediments of fluvial and marine origin and has diverse landforms, such as paleochannels, tidal islands, mangrove swamps, and strandlines. The deltaic region is a gently rolling low lying plain with a general slope towards the south and south-east. The palaeochannels are characterized by coarse sediments and the flood plains with alternations of coarser and finer clastics.

Being spread over the Indian Peninsula, monsoon has dominant control over the climate of the basin. Headwater (and downstream) portions of the basin receive comparatively higher amounts of rainfall during southwest (and northeast) monsoon periods, compared to the inland areas. The mean annual rainfall of the basin is 840 mm (Biggs et al., 2007), of which roughly 90% occurs from May to October (Jain et al., 2007). Gunnell (1997) observed a dramatic decrease of annual rainfall from 3000 mm (in the Western Ghats) to about 500 mm over a distance of 80 km east of the Western Ghats. Similarly, annual rainfall (gradually) decreases from about 1000 mm in the deltaic region in the east to nearly 500 mm in the northwestern parts of the basin. The long-term mean annual surface flow of the KRB is 78 km^3, of which 58 km^3 is considered to be utilizable (Amarasinghe et al., 2005). High flows in the river occur during the months of August to December, while the lean flow season is from April to May (Jain et al., 2007). The basin consists of 660 dams, 12 barrages, 58 weirs, 6 anicuts and 119 lifts (MoWR, 2014). Water resources of the basin are mostly utilized for irrigated agriculture, followed by hydroelectric power generation. River discharge has been decreased rapidly during 1960–2003 due to the expansion of irrigation projects, leading to basin closure (Biggs et al., 2007), where the dams and reservoirs along with other minor irrigation schemes store about 54 billion m^3 of water, which is 95% of the pre-1965 runoff, when few dams were in existence (Venot, 2009).

The basin supports numerous vegetation types, where cropland is the dominant land use type and accounts for about 82% of the basin area. About 6% of the area is covered by scrublands, grasslands, and savannahs with sparse vegetation cover, while another 1% area is characterized as different types of forest (mostly along the slopes of the Western Ghats). Roughly 2% of the basin area is classified as urban and built-up land use types, which are spatially evenly distributed across the basin.

Table 1
Details of the study reaches of the Krishna River.

Reach-ID	Length (km)	Average width (m)	Slope (m m^{-1}) [a]
R1	50	429	0.58
R2	50	521	0.26
R3	50	1144	0.04
R4	50	3044	0.32
R5	50	3234	0.14
R6	43	1621	0.02
R7	11	777	0.02
R8	14	664	0.01

[a] The slope is represented as the drop in the elevation between the source and the end of the river reach over the reach length. The hydrologically-corrected SRTM DEM (1 arc-second) was used to estimate the elevation of the source and end points.

3. Materials and methods

3.1. Satellite data and preprocessing

The present study has made use of multi-temporal Landsat data (for the years 1973, 1991 and 2015) to assess the bank line changes, if any, occurred in the lower reaches of the KRB. Satellite images for the different years for the study region were downloaded from USGS Earth Explorer (https://earthexplorer.usgs.gov). For the year 1973, Multispectral Scanner System (MSS) data were used, while Thematic Mapper (TM) data were used for the year 1991, and the data for the year 2015 were from Operational Land Imager (OLI) (Table 2). Owing to the excessive coverage of clouds on the scenes during the monsoon season, the dry season (preferably during February and March) images with cloud cover less than 10% were considered. The downloaded scenes were preprocessed to reduce sensor and atmospheric noises using haze and noise reduction and histogram equalization algorithms using ERDAS Imagine.

3.2. Delineation of channel banks

The reliability of the assessment of temporal changes of channel bank line depends on the accuracy of river channel boundaries extracted from the satellite data (which in turn to the resolution of the sensor). Yet, the delineation of accurate channel bank lines is a challenging task, regardless of the numerous methods ranging from automated classification to manual digitization. The major drawback of the automated classification procedure is the inconsistencies due to the similarities in spectral reflectance between the riverine and associated features. Although there exist automated methods for extracting rivers and lakes from Landsat images (Jiang et al., 2014), most of the channel morphological studies recommended manual digitization for delineation of river banks from multispectral data (e.g., Yang et al., 1999; Yao et al., 2011; Gupta et al., 2013; Dewan et al., 2017). Following this, the channel bank lines of the lower reaches of the Krishna River were manually digitized from the Landsat images of different years using multi-band combinations.

Even though the land-water boundary was evident for most of the

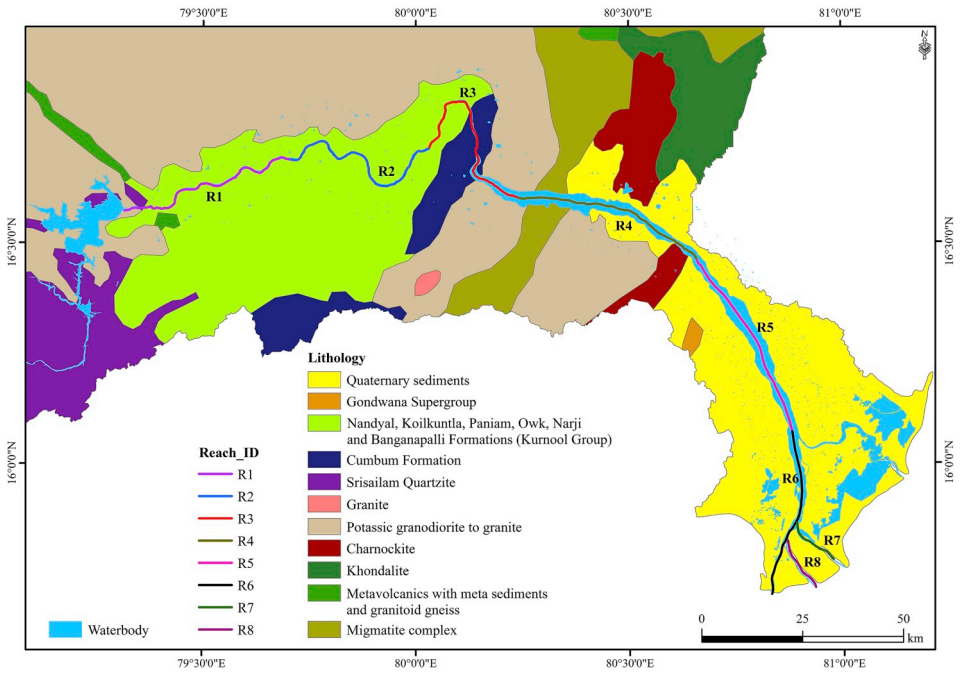

Fig. 2. Lithology of the study reaches of the Krishna River (Source: Geological Survey of India).

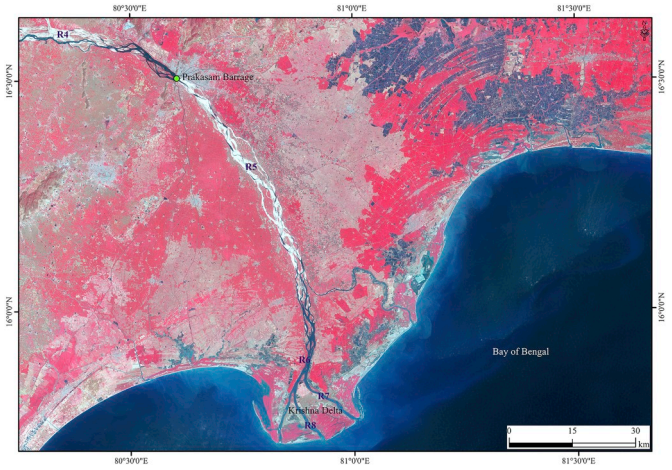

Fig. 3. Landsat 8 OLI image of the lower reaches (R4 to R8) of the Krishna River.

river reaches in the satellite images, varying water levels in the river channels and masking of the banks by riparian vegetation canopy made identification of channel bank line difficult in some reaches. Hence, we adopted the soil-vegetation limit approach (Gurnell, 1997) to identify the bankfull channel boundary, where the river channel was defined as the area with vegetation cover less than 10% (Lawler, 1993; Tiegs and Pohl, 2005). This approach has been proved as an efficient method for delineating channel boundaries by several researchers (e.g., Gurnell, 1997; Winterbottom, 2000; Richard et al., 2005; Yao et al., 2011; Hossain et al., 2013). In addition, the prominent changes in the slope of the transverse valley profiles (derived from 1 arc-second SRTM DEM) were also used for the delineation of bank lines.

3.3. Estimation of erosion and deposition areas

The bank lines delineated from the images of the years 1973, 1991 and 2015 were compared to estimate the areal extent of the erosion and deposition areas during 1973–1991 and 1991–2015. The delineated left and right bank lines of the different years were merged into a single feature class in ArcGIS and created the polygons that represent the difference between the bank lines. While comparing the changes in the bank lines between 1973 and 1991, 1973 was taken as the reference bank line, and the polygons (created by merging 1973 and 1991 bank lines) were classified into erosion and deposition, depending on the location of the polygons with respect to the reference year. For example, for the left bank, the polygons left to 1973 bank line represent erosion, and the polygons right of the bank line indicate deposition. The same process was used to characterize erosion and deposition polygons on the right bank, but with the following change: polygons to the left and right of 1973 bank line represent deposition and erosion, respectively. Area of the polygons was calculated, and summation of the area of the polygons provided the total area under bank erosion and deposition during the period. Similar steps were repeated to quantify the total area of erosion and deposition during 1991–2015.

Daily gauge and discharge data from two hydrological observatories (HO 1 in R1 and HO 2 in R3; Fig. 1) were collected from the Central

Table 2
Remote sensing images used for delineation of bank lines of the lower reaches of the Krishna River.

Landsat 1 MSS		Landsat 5 TM		Landsat 8 OLI	
Spatial resolution = 60 m[a]		Spatial resolution = 30 m		Spatial resolution = 30 m	
Spectral resolution = 4		Spectral resolution = 7		Spectral resolution = 11	
Path/ Row	Date of acquisition	Path/ Row	Date of acquisition	Path/ Row	Date of acquisition
152/ 049	20-01-1973	142/ 048	18-03-1991	142/ 048	05-04-2015
153/ 048	26-02-1973	142/ 049	18-03-1991	142/ 049	20-03-2015
153/ 049	26-02-1973	143/ 048	25-03-1991	143/ 048	27-03-2015
154/ 048	27-02-1973	143/ 049	25-03-1991	143/ 049	27-03-2015
154/ 049	27-02-1973				

[a] Original MSS pixel size was 79 × 57 m, but resampled to 60 m.

Water Commission (CWC). The hydrological data were analyzed to assess the role of floods on bank erosion. The gauge station HO 1 is located at Pondugala (79° 39′ 32″ E, 16° 41’ 2″ N), downstream of the Nagarjuna Sagar Dam and Nagarjuna Sagar Tail Pond Dam, and HO 2 is at Wadenapalli (80° 9′ 49″ E, 16° 45′ 23” N), downstream of Pulichintala Dam. The CWC stations have different lengths of data record: 32 years (1975–2007) at HO 1, and 50 years (1965–2015) at HO 2. In order to evaluate the geological controls on bank erosion, lithological types of the study region were extracted from the geological and mineral map of Andhra Pradesh and Telangana States (Source: Geological Survey of India; 1:2,000,000).

4. Results

The bank lines of the lower reaches of the KRB delineated from the Landsat images were used to estimate the mean width of the river reaches during the respective years. Fig. 4 indicates significant spatial variability in the mean width of the river reaches with an irregular downstream trend with a peak at R5. The reaches, R4 and R5 are remarkably wider than the rest of the reaches, where the mean width of these reaches exceeds 2500 m. Contrary to the general increasing downstream trend of river width (due to increasing discharge), the mean width of the study reaches shows an increasing trend up to R5, followed by a decreasing trend. The increasing trend of the upper reaches, especially between R1 and R5, implies the topographic controls (e.g., incision) on channel development. The transverse profiles (derived from 1 arc-second SRTM DEM) drawn along the transects at R2 and R4 demonstrate the contrasting nature of topographical settings, i.e., the confined channel boundary in R2 vs. the unconfined channel of R4 (Fig. 4). Being developed in the eastern coastal plains, the elevation gradient across the valley of R4 is significantly smaller, compared to R2. The reaches downstream of R5 exhibit a decreasing trend, which reflects the bifurcation of the distributaries in the Krishna Delta. However, the variability of the mean width of the river reaches between the years is not significant in the study reaches.

Bank erosion and deposition in the study reaches during 1973–1991 and 1991–2015 were estimated using the bank lines of different years (Fig. 5), and the results are discussed in the following sections.

4.1. Erosion along the banks

Analysis of the bank line changes occurred during 1973–1991 indicated that the total area of bank erosion was 3093 ha, of which 58% (1792 ha) was contributed by the left bank, and 42% by the right bank (1301 ha). The area of erosion along the left bank of the study reaches

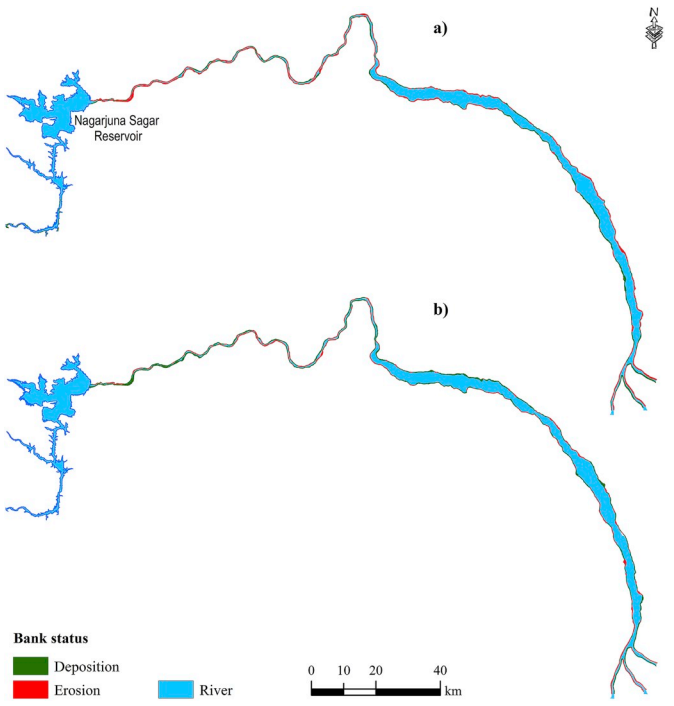

Fig. 5. Spatial pattern of bank erosion and deposition along the study reaches during (a) 1973–1991 and (b) 1991–2015.

varied between 133 ha and 439 ha, while along the right bank, it showed a range between 1 ha and 494 ha (Fig. 6a). The areal extent of erosion along the left and right banks of the reaches showed significant spatial variability within and between the reaches (Fig. 7a), and the maximum rates of bank erosion for the left and right banks were observed in R5 (i.e., 439 ha) and R1 (i.e., 494 ha), respectively. Downstream variation of bank erosion along the left bank showed an increasing trend till R5, and subsequently decreases, whereas bank erosion along the right bank exhibited an irregular, but decreasing trend (Fig. 6a).

The mean width of bank erosion was estimated by dividing the cumulative area of bank erosion of any given reach with the length of the reach. Similar to the variability in the area of erosion, the mean width of erosion during 1973–1991 also had considerable spatial variability across the reaches (Fig. 6b). The erosion width along the left bank varied between 27 m and 121 m, whereas the maximum erosion width was observed to be ~100 m along the right bank. The maximum width of

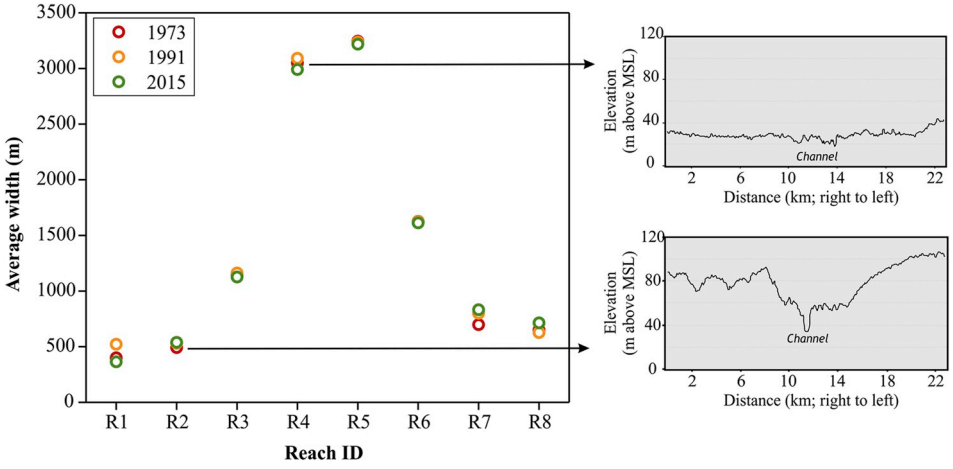

Fig. 4. Mean width of the lower river reaches of the Krishna River during 1973, 1991 and 2015 estimated from Landsat images. Cross-section profiles drawn along the transects (from right to left) at R2 and R4.

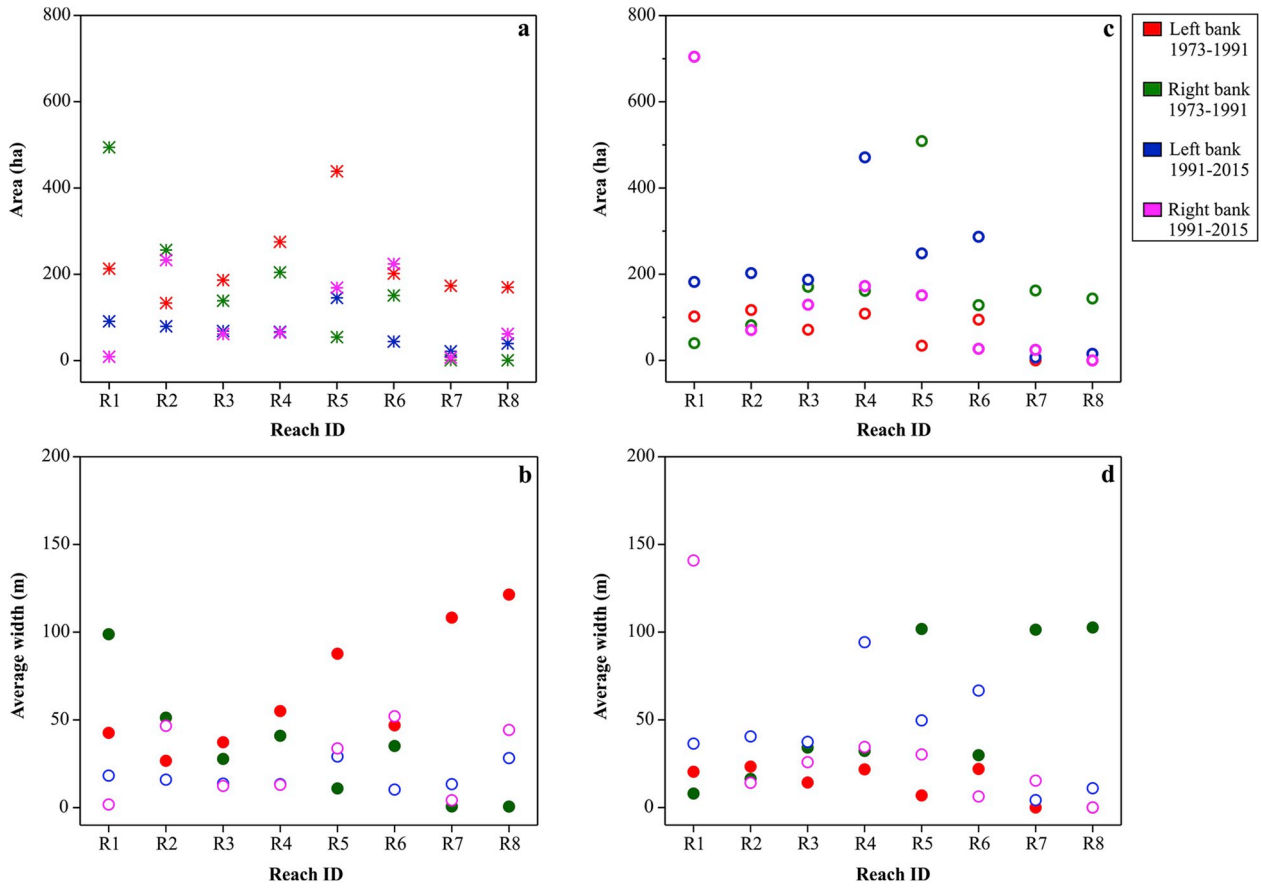

Fig. 6. Variability in the erosion and deposition along the left and right banks during 1973–1991 and 1991–2015: (a) total area of erosion, (b) average width of erosion, (c) total area of deposition and (d) average width of deposition.

erosion along the left bank was measured in R8 (121 m) and R7 (108 m), which are located in the deltaic region. However, the erosion width of these reaches along the right bank was significantly low. Although the area of bank erosion of these reaches was comparably smaller than the other reaches of the downstream region (Fig. 6a), the differences between the area and mean width of erosion along the left bank of these reaches are due to the high erosion intensity over shorter lengths (11 and 14 km, respectively for R7 and R8; Table 1). On the other hand, along the right bank, the mean width of bank erosion was high in R1 (99 m), followed by R2 (51 m) and R4 (41 m). The mean width of bank erosion demonstrated contrasting downstream trends between the banks, where the left bank showed an increasing trend, while a decreasing trend for the right bank.

The bank line changes during 1991–2015 suggested that a total of 1386 ha area was eroded during the period, where bank erosion was relatively higher along the right bank (830 ha), compared to the left bank (556 ha). The areal extent of bank erosion along the left bank of the reaches varied between 21 ha (R7) and 145 ha (R5) (Fig. 6a). However, along the right bank, variation in the estimated area was between 7 ha (R7) and >200 ha (R2 and R6). Although the area of bank erosion along the left bank showed a general decreasing trend towards downstream (with an exception in R5), hardly any trends were observed along the right bank. The intra- and inter-reach variability in the area of erosion patches along the banks were high during 1991–2015 also (Fig. 7b). During 1991–2015, the mean width of erosion along the left and right banks ranged from 10 m (R6) to 29 m (R5) and 2 m (R1) to 52 m (R6), respectively (Fig. 6b). The spatial variability of the mean width of erosion along the banks during 1991–2015 was remarkably lower, compared to the period 1973–1991.

On a mean annual basis, nearly 94 ha land area was eroded along the left bank during 1973–1991, whereas it was 68 ha along the right bank. However, the annual rates of erosion along the left and right banks were remarkably low during 1991–2015 (23 ha and 35 ha respectively). The analysis indicated that the area of erosion along the left bank of the reaches was relatively higher during 1973–1991. However, along the right bank, erosion rates of the upper reaches (R1 to R4) were comparatively higher during 1973–1991, while the lower reaches are characterized by relatively higher rates of erosion during 1991–2015. Six of the eight reaches (i.e., R3 to R8) are characterized by relatively higher erosion along the left bank during 1973–1991, whereas only four reaches had higher erosion rates along the left bank during 1991–2015 (i.e., R1, R3, R4, and R7). It is also noted that a few reaches did not show hardly any changes in the erosion dominance along the banks between the assessment periods, e.g., R2 had relatively higher erosion along the right bank during 1973–1991 and 1991–2015, whereas erosion along the left bank of R3, R4 and R7 was dominant during both the periods.

4.2. Deposition along the banks

The total area under deposition along the banks during 1973–1991 was 1924 ha, where 527 ha was along the left bank and 1397 ha was along the right bank. The individual reaches showed substantial variability for deposition along the left (<1–117 ha) as well as right banks (39–509 ha; Fig. 6c). Similar to the variability in the area of erosion patches of the reaches, the depositional patches of the various reaches also exhibited huge variability (Fig. 7c). Further, the mean width of deposition along the left and right banks varied from <1 m to 23 m and 8 m–103 m, respectively (Fig. 6d). In general, the deposition rate was relatively higher along the right bank, compared to the left bank.

During 1991–2015, the total area under deposition along the entire

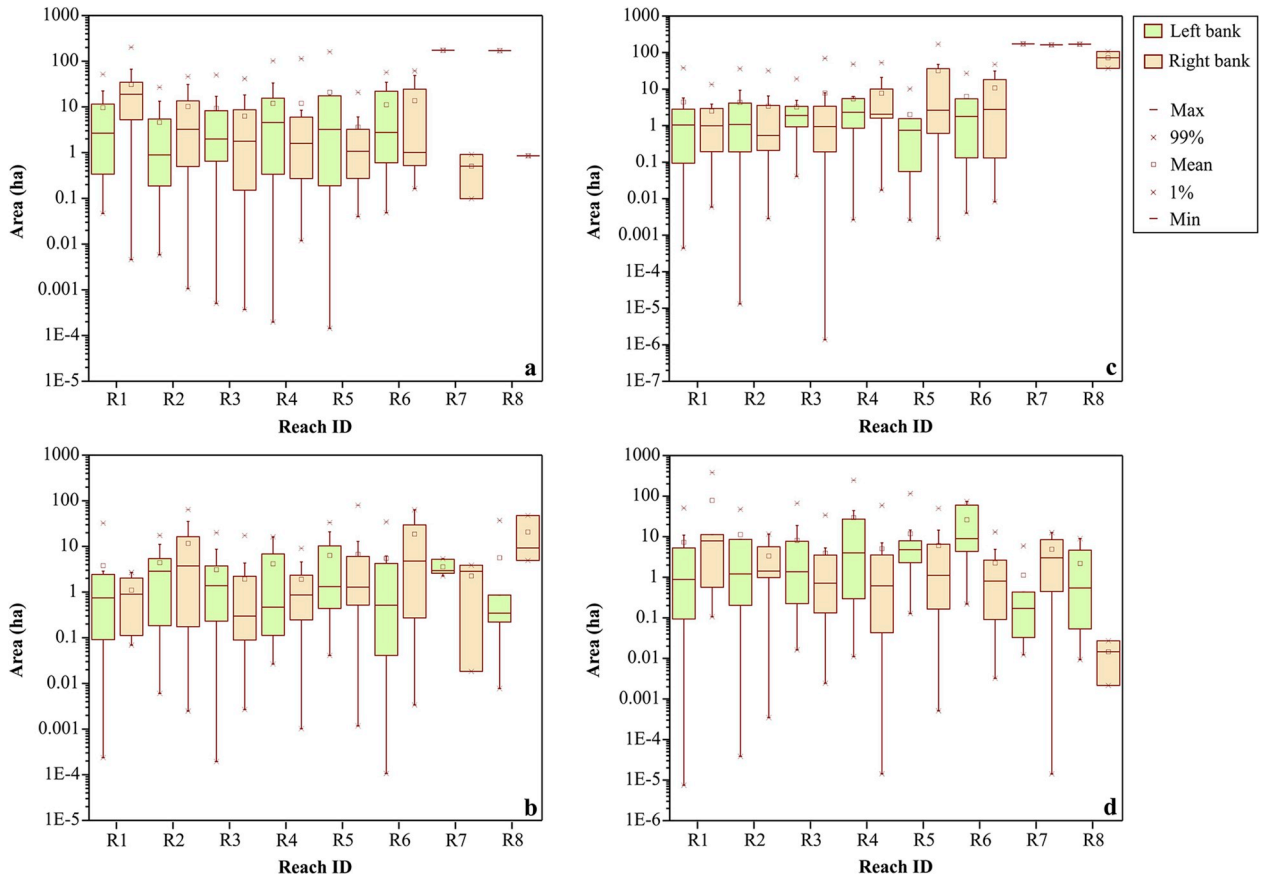

Fig. 7. Summary statistics of the variability in the areal extent of the erosion and deposition patches along the banks: (a) and (c) represent erosion and deposition occurred during 1973–1991 and (b) and (d) represent erosion and deposition occurred during 1991–2015.

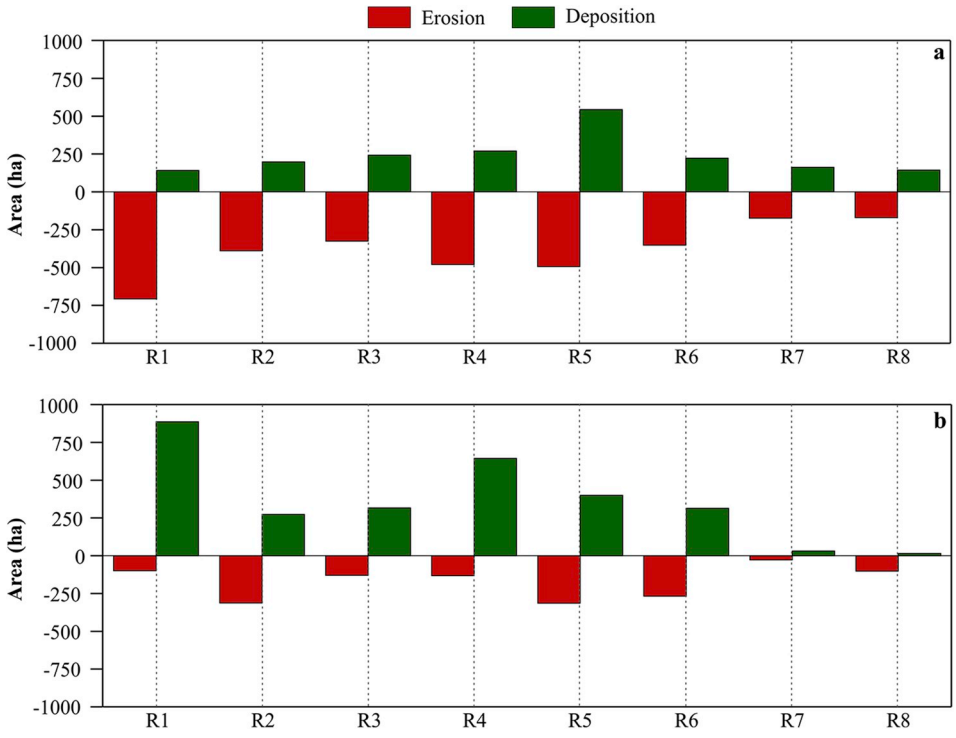

Fig. 8. Comparison of total erosion and deposition pattern (inclusive of both banks) across the study reaches during (a) 1973–1991 and (b) 1991–2015.

reaches was 2880 ha, of which 1600 ha was contributed by the left bank and 1280 ha by the right bank. Among the reaches, R1 to R6 showed a significantly higher areal extent of bank deposition, compared to R7 and R8 (Fig. 6c), which was true for both the left and right banks. The maximum depositional area along the banks was developed in R1 and R4, whereas the reaches of the deltaic region were characterized by their significantly smaller areal extent of bank deposition. Moreover, the area of the depositional patches of the individual reaches showed remarkable spatial variability (Fig. 7d).

The annual rates of deposition of the study reaches during 1973–1991 suggested that, on a mean annual basis, 28 ha of the area was developed as a result of deposition along the left bank, whereas 74 ha of land was developed along the right bank. However, during 1991–2015, the areal extent of deposition per year along the left bank was increased to 67 ha, whereas decreased along the right bank (i.e., 53 ha).

4.3. Erosion vs. deposition along the banks

The erosion and deposition (of both the banks) of the individual reaches were compared to understand the spatial pattern of the erosion and deposition processes that occurred during 1973–1991 and 1991–2015. Fig. 8 suggests that bank erosion was predominant in most of the reaches during 1973–1991, compared to bank deposition, whereas the pattern was reversed during 1991–2015, i.e., the rate of deposition was higher compared to erosion. On a mean basis, the rate of erosion of the reaches during 1973–1991 was roughly twice the rate of bank deposition, while it was only 1.4 times the rate of bank deposition during 1991–2015.

Although the magnitude of the bank line shifts was small, the estimates of the total erosion and deposition along the left and right banks of the individual reaches during the assessment periods implied that R2 and R6 shifted their left bank towards the channel thalweg, whereas right bank shifted away from the thalweg. On the contrary, R1, R5, R7, and R8 shifted their left bank away from the thalweg, and right bank towards the thalweg. The left bank of R3 showed hardly any changes, while the right bank moved towards the channel centre. The reach, viz., R4 exhibited shifting of both channel bank lines towards the thalweg.

The scale of data capture is a major issue that seriously affects delineation of channel boundary while using multi-temporal remote sensing data (Tiegs and Pohl, 2005; Rozo et al., 2014).

The remote sensing data used in this study were of different spatial resolutions. The spatial resolution of the Landsat 1 MSS images (1973) was 60 m, whereas the spatial resolution of the Landsat TM (1991) and OLI (2015) images was 30 m. Hence, the changes in bank lines with a magnitude of less than 60 m may not be recognized during 1973–1991, and a change of less than 30 m may not be detected during 1991–2015. Even though the mean width of erosion and deposition of the left and right banks during 1973–1991 and 1991–2015 exhibits wide variability (Fig. 6 b, d), the lower values than the aforementioned thresholds could mostly be the result of the errors during the delineation of bank lines.

4.4. Degree of braiding

The planform of the upper reaches is more or less straight to sinuous channels, while the downstream reaches of the Krishna River (R4 to R6), except the distributaries, are braided. The intensity of braiding was assessed by estimating the planform index (PFI; Sharma, 1995) during 1973, 1991 and 2015 using Eq. (1):

$$PFI = \frac{\frac{T}{B} \times 100}{N} \quad (1)$$

where, T is sum of the flow top widths of all the braided channels, B is overall flow width and N is the number of braided channels. The PFI implies the fluvial landform disposition with respect to a given water level, and a lower PFI value is indicative of a higher degree of braiding. Five transects at defined intervals (10 km) were drawn in each of the braided reaches to estimate the PFI of each transect, and the PFI value of the reach was calculated as the mean value of the PFI values of different transects of a given reach.

Table 3 is the estimated PFI values of the braided reaches during 1973, 1991 and 2015. Among the different braided reaches, R5 has comparatively lower PFI values in all the years, followed by R4 and R6. Sharma (2004) classified the PFI values of the channels into highly braided ($PFI \leq 4$), moderately braided ($19 \geq PFI > 4$) and low braided ($PFI > 19$). Following the classification, R4 and R5 are moderately braided, whereas R6 belongs to the low braided class. However, the variability in PFI of the reaches was considerably small among the years.

5. Discussion

Analysis of the changes in bank lines of the lower reaches of the Krishna River indicated that the erosion and deposition along the banks are highly varying across space and time. The individual reaches (R1 to R8) showed significant variability in the erosion as well as deposition patterns between the time periods (i.e., 1973–1991 and 1991–2015). It is well established that various natural and anthropogenic drivers, such as floods, modification of land use/land cover, and flow regulation are significant in controlling erosion along river banks (Rinaldi, 2003; Gregory, 2006; Radoane et al., 2013; Morais et al., 2016). Hence, the effects of floods and flow regulation (by the Nagarjuna Sagar Dam) on bank erosion are discussed in the following paragraphs. The lithology of the area varies considerably, and hence, geological controls on bank erosion are also addressed. Since the reaches, R4 to R6 are braided, the discussion is extended to the effect of braiding on the bank erosion and deposition in the braided reaches.

5.1. Influence of floods

Since changes in water and sediment discharge are the major factors affecting channel geometry and morphology of alluvial rivers (Merritt and Wohl, 2003), flood events can trigger abrupt changes in the river channel geometry. The daily discharge time series of two HO stations (HO 1 in R1 and HO 2 in R3) along with the flood discharge magnitudes of different return periods are shown in Fig. 9. Frequency analysis of the discharge data was performed by fitting Generalized Pareto Distribution to all the peak events above a fixed threshold, which is a widely used threshold selection criteria based on mean residual life plot (Coles, 2001, 80 p.). The fitted Generalized Pareto Distribution was tested for goodness-of-fit using Anderson Darling, Kolmogorov-Smirnov, and Chi-square tests, and all the three tests indicated the goodness of fit at 5% significance level.

Since the flow regime of the Krishna River is highly regulated, changes in the channel morphology as a result of the flood events could have been less obvious. However, the steeper slopes of the high-flow of the monthly flow duration curves imply the significance of rain-induced floods on the river discharge (Fig. 10). The high-magnitude flood event recorded at HO 1 ($31018\ m^3\ s^{-1}$) was during October 1998 (with a recurrence interval more than 100 years), whereas the high-magnitude flood event recorded at HO 2 ($31803\ m^3\ s^{-1}$) was during October 2009 (with a return period of 319 years). Since the length of the data of HO 1

Table 3
Mean PFI of the braided reaches of the Krishna River during different years.

Year	R4	R5	R6
1973	15.8 (8.3–30.5)	8.8 (6.3–13.9)	68.7 (7.7–100)
1991	18.9 (9.1–26.3)	9.5 (6.5–12.6)	58.2 (7.8–100)
2015	12.4 (6.3–24.5)	10.6 (4.3–16.0)	58.2 (8.3–100)

Value in parentheses is the range of PFI values of the transects in the corresponding reaches.

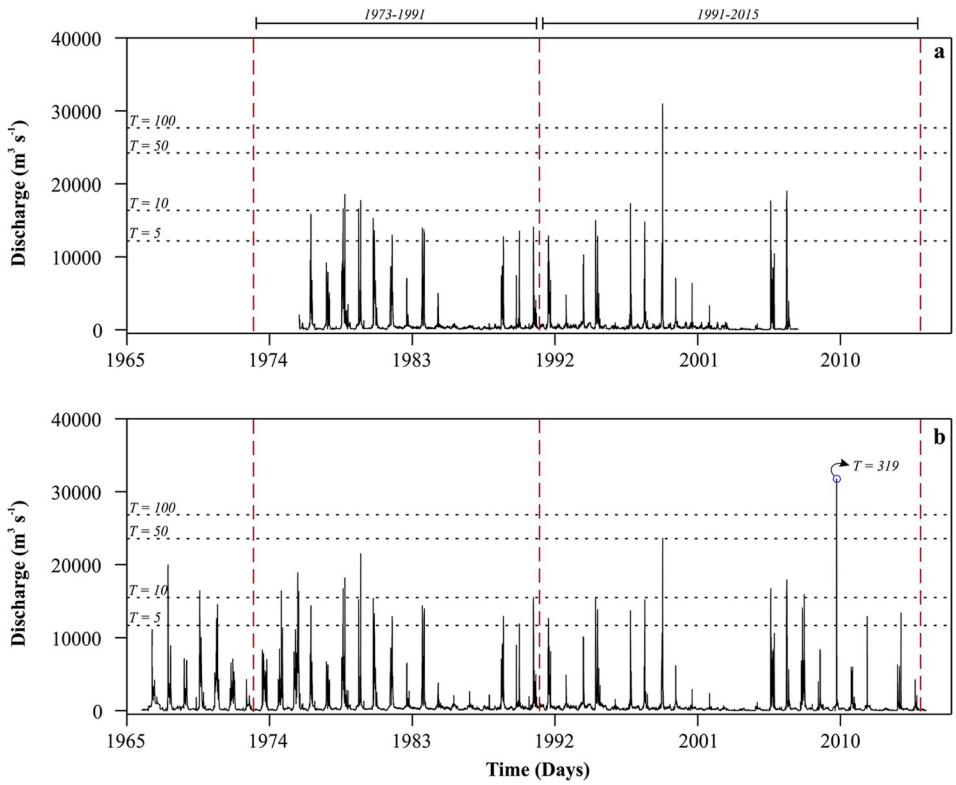

Fig. 9. Daily discharge at (a) HO 1 and (b) HO 2, including the flood discharges of 5-, 10-, 50- and 100-year return periods (T). Refer Fig. 1 for the geographic coordinates of the HO stations.

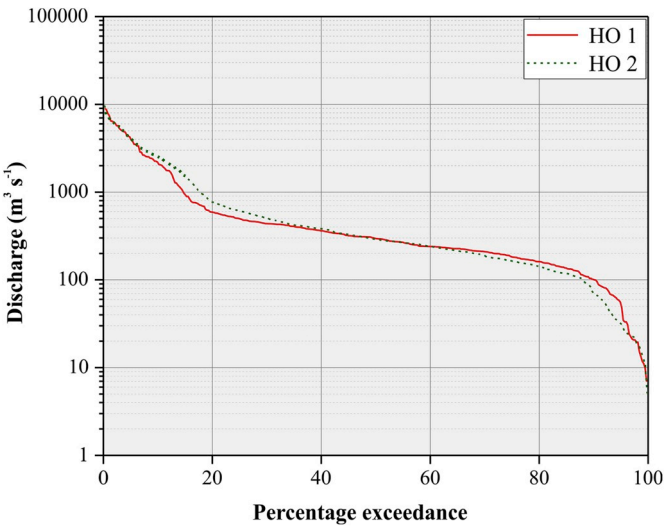

Fig. 10. Mean monthly flow duration curves for HO 1 and HO 2.

was only up to 2007, the 2009 flood event was not reflected in the time series. The 2009 flood event was severe in the lower reaches of the Krishna River, and the flooding had resulted in the physical changes of the river channel and the banks, including extensive bank erosion, breach of levees, winnowing of finer sediments and removal of vegetation (APWRDC, 2009). The observations of Couper and Maddock (2001) is pertinent in this context, where the assessment of bank erosion during the pre- and post-flood event evidently indicated that the flood event caused to increase bank erosion significantly. The study showed that the subaerial processes alone yielded erosion rates ranging from 0 to 181 mm a^{-1}, with a mean of 32.6 mm a^{-1}. However, the inclusion of the effects of the flood event increased the range of erosion rates to 2.8–356 mm a^{-1}, with the mean, 59.8 mm a^{-1}.

A comparison of the time series of daily flows suggested that flood events of larger return periods were recorded during 1991–2015 in both the HO stations, compared to 1973–1991 (Fig. 9). Since the record length of HO 1 (1975–2007) did not cover the channel bank assessment period (i.e., 1973–2015), discharge data of the station were not used for detailed analysis. Fig. 9 clearly suggests that HO 2 witnessed a greater number of flood events (of return period of more than 5 years) during 1973–1991, compared to 1991–2015. Statistically, channel-forming discharge is a more reliable measure for hydraulic geometry relations. Simon et al. (2016) proposed that the channel-forming discharge has a return period of 1.5 years. The channel-forming discharge (with recurrence interval 1.5 years) at HO 1 was 4407 $m^3 s^{-1}$, whereas, at HO 2, it was 4799 $m^3 s^{-1}$. The number of flood events recorded HO 2, whose magnitudes greater than the channel-forming discharge was estimated for 1973–1991 and 1991–2015. It may be noted that the total number of flood events was relatively higher during 1973–1991, compared to 1991–2015: 40 flood events occurred during 1973–1991 indicating an average of 21 events in 10 years, while only 31 events during 1991–2015 suggesting an average of 13 events in 10 years. This is evident in Fig. 11, which demonstrates that 1973–1991 was characterized by frequently occurring, low magnitude flood events, while 1991–2015 has infrequent, high magnitude floods (such as the flood in 2009).

Flood duration has a significant role in determining bank erosion, as Simon et al. (1999) observed that the highest rates of bank retreat occur as a result of high flows during prolonged wet periods. Hence, the duration of the flood events was also compared between the periods. The analysis suggested that the length of the events that occurred during 1973–1991 (mean = 5 days) was comparatively higher than the events during 1991–2015 (mean = 4 days). Hence, it may be inferred that the higher rate of bank erosion along the lower reaches of the Krishna River during 1973–1991 (compared to 1991–2015) could be a reflection of the increased number of flood events with a relatively longer duration.

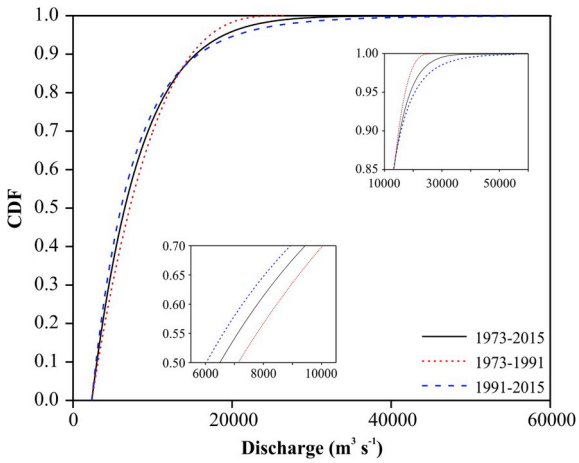

Fig. 11. Cumulative distribution function of the discharge data at HO 2 for the entire period (1973–2015) as well as for 1973–1991 and 1991–2015. Inset is the enlarged sections between CDF 0.5 and 0.7 as well as 0.85 and 1.0.

5.2. Impacts of hydraulic structures

Hydraulic structures, such as dams induce changes in the primary fluvial processes downstream of the structures causing adjustments of channel form (Petts and Gurnell, 2005). The water released from the large dams is nearly devoid of suspended sediments, and the sediment-starved dam releases are conducive to entrap channel bed and bank sediments (Hupp et al., 2009). The major hydraulic structures of the reaches are the Nagarjuna Sagar Dam and the Nagarjuna Sagar Tail Pond Dam (in R1), the Pulichintala Dam (in R3) and the Prakasam Barrage (in R4). Among the four structures, the major structure is the Nagarjuna Sagar Dam, which was completed in 1974. The dam has a length of 4865 m, and a height of ~125 m and the reservoir submerged an area of 28500 ha (MoWR, 2014). Being one of the largest dams of the basin, the impact of the Nagarjuna Sagar Dam on bank erosion in the reaches R1 to R3 was assessed, whereas the Nagarjuna Sagar Tail Pond and the Pulichintala dams were not considered as these dams were completed after 2010.

Area of erosion along both the banks of the study reaches (R1 to R3) immediately downstream of the Nagarjuna Sagar Dam was estimated during 1973–1991 and 1991–2015. For this, the areal extent of erosion was estimated at every 5 km interval of the reaches (i.e., 30 segments) (Fig. 12). The spatial pattern of the bank erosion evidently indicated a sharp increase in the area of bank erosion downstream of the dam and is prominently visible during 1973–1991 (from ~50 ha to ~200 ha in a length of 10 km). The increased areal extent of bank erosion downstream of the dam can be ascribed as an effect of river regulation. However, the effect of the dam on the magnitude of bank erosion was not significant during 1991–2015, while compared with 1973–1991. It may be noted that the dam was completed in 1974, and therefore, the effect of river regulation would have been manifested significantly during the 1973–1991 period. Erosion immediately below dams has been reported by various researchers (e.g., Petts, 1979; Shields et al., 2000; Phillips et al., 2004; Yang et al., 2007), and Zhang et al. (2016) suggested that the erosion was increased since the construction of the Three Gorges Dam. Prior to completion of the dam, the eroded sediment in the reach was $6.67 \times 10^4\ m^3\ km^{-1} \cdot yr^{-1}$, whereas the initial stage (2003–2006), transitional stage (2006–2008), and normal stage of the project recorded sediment erosion levels 21×10^4, 12.6×10^4 and $20.8 \times 10^4\ m^3\ km^{-1} \cdot yr^{-1}$, respectively.

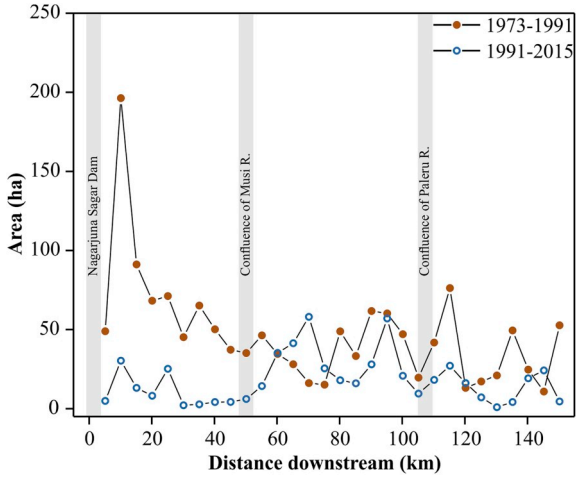

Fig. 12. Spatial variation of bank erosion downstream of the Nagarjuna Sagar Dam (R1 to R3) during 1973–1991 and 1991–2015.

Bank erosion along the reaches showed an irregular trend after the sudden increase downstream of the dam during both the assessment periods (Fig. 12). Although bank erosion downstream of the dam is significantly high, bank erosion also peaks between 60 and 120 km downstream of the dam. It may be noted that the segments characterized by elevated levels of bank erosion represent channel sections downstream of the confluence with major tributaries. For example, the Musi River joins the Krishna River nearly 50 km downstream of the Nagarjuna Sagar Dam, and the Paleru River meets the Krishna River roughly 110 km downstream of the dam.

The left bank of the extreme lower reaches, viz., R6 (partly), R7 and R8, in the Krishna Delta, experienced severe erosion and the right bank was subjected to deposition during 1973–1991 (Fig. 6a, c). Contrastingly, relatively higher rates of erosion along the right bank and larger rates of deposition along the left bank characterize these reaches during 1991–2015. It was reported that the substantial rates of erosion along the channel segments in the deltaic region were the result of decreasing discharge and basin closure due to the construction of vast numbers of water resources projects since 1960. (e.g., Biggs et al., 2007; Gamage and Smakhtin, 2009; Rao et al., 2010). Prior to 1960, hardly any major projects exist across the Krishna as well as the Tungabhadra (a major tributary of the Krishna River) other than the Prakasam Barrage and the Tungabhadra Dam. However, analysis of the discharge data (Rao et al., 2010) indicated that the annual discharges reflect the impact of the major dams, such as the Nagarjuna Sagar Dam, recording a substantial dip in discharge level in the years after the construction of the dam.

5.3. Effect of braiding

The study reaches, R4 to R6 experienced significant erosion as well as deposition along the banks during both the periods (Fig. 8), implying the dynamic nature of the channels. This may be correlated with the braided nature of the study reaches (Fig. 3), as the deflection of the channel flows around the developed sand bars could be a primary cause of bank erosion and associated channel widening. In the Brahmaputra River, Akthar et al. (2011) observed that bank erosion along the braided reaches was induced by the flow concentrations due to the temporal evolution of multiple channels. Thorne et al. (1993) also identified bank migration processes, which are driven by bar development and migration in braided reaches operating at smaller spatial (3–6 km) and over shorter temporal scales (2–5 years). However, Ta et al. (2013) reported that the braided channel in the sand-banked reach of upstream of the Yellow River was characterized by an increasing trend in both channel deposition and lateral channel erosion in response to decreased flows. It is further explained that erosion from toes of the channel bank causes bank failure, delivering excess volumes of sediment into the central portion of the channel, and thereby developing a bank-to-channel sediment transfer. This could have been a potential mechanism for the relatively higher rates of bank erosion as well as deposition along the braided reaches of the Krishna River.

5.4. Geological controls

The topography and geological setting exert significant controls on the changes in channel geometry and morphology (Booth and Henshaw, 2001; Tooth et al., 2002). The nature of the geologic substrate strongly affects the susceptibility of the channel to change. The reaches, lower part of R4 to R8 are solely developed on the Quaternary sediments, whereas R1 to R4 are formed mostly on the rocks of Kurnool Group and Cumbum Formation, peninsular gneisses, charnockite, migmatite complex and quartzite (Fig. 2). In order to analyze the effect of lithology on bank erosion, erosion along the banks between 1973 and 2015 was estimated with respect to lithological types.

It is evident that bank erosion in the lower reaches (especially developed in the Quaternary sediments) is considerably higher, compared to other lithological types (Fig. 13). Field observations indicated that the rocks of the Kurnool Group (consisting mainly of limestone, slate, and quartzite) are stratified and highly jointed, where erosion occurs primarily along the lines of weakness, such as joints or fractures. In the reaches dominated by the rocks of the Kurnool Group (e.g., R1 to R3), vertical erosion may be dominated over lateral erosion leading to confined valleys, which is supported by the transverse profile at R2 (Fig. 2). On the other hand, erosion in the Quaternary sediments is primarily a function of the erodibility and shear strength of the bank matrix, and the high erosion intensity is the result of the weak bank resistance of the unconsolidated substrate. This is supported by the observations of Tooth et al. (2002), where a significant difference in the channel and floodplain morphology was observed between sandstone and dolerite lithology, i.e., significant meandering occurs in sandstone lithology, while the channel course on dolerite is essentially straight with the absence of (or lean) floodplains. Further, analysis of the spatial variability of mean width of the river reaches (Fig. 4) along with geological map (Fig. 2), also indicated that the marked variations in the mean width of the reaches are strongly linked with variations in lithology, specifically from the rocks of Kurnool Group, Cumbum Formation and peninsular gneisses to Quaternary sediments.

The analysis of the major drivers of bank erosion evidently indicated that floods, river regulation, and regional geology have significant controls in determining erosion along the banks of the lower reaches of the Krishna River. This holds further implications for the identification of spatial variations in the process dominance and individual contributions of the process domains.

In India, most of the studies related to fluvial geomorphology have been carried out in the Himalayan Rivers, where numerous research works are available on different aspects of river channel morphology as well as the controls exerted by various fluvial-hydrological-processes and the geomorphic implications of regional tectonics. The results of the present study are compared with a few channel morphological investigations carried out in the regional context. Goswami et al. (1999) studied the sequential changes in the position of bank lines as a result of bank erosion in the Subansiri river in Assam using Survey of India topographic maps (1:63,360 and 1:50,000 scales) and IRS LISS III images. The study suggested that the total amount of bank area eroded along the entire river course of the Subansiri River in Assam under the study during 1920–1970 and 1970–1990 was 107.90 and 57.50 km^2 with the average annual rates of 2.16 and 2.88 km^2, respectively. Similarly, the study of Sarma (2005) on bank erosion of the Brahmaputra River within Assam during the twentieth century estimated that the total area eroded in north and south banks was 782.49 km^2 and 747.61 km^2 (total 1530.10 km^2), respectively. The net effect was a loss of 979.94 km^2 total bank area from a 630 km length of the Brahmaputra River in Assam.

Sarma and Acharjee (2012) studied the sequential changes in the position of bank lines of the Brahmaputra River due to consistent bank erosion using Survey of India topographic maps of 1912–1916 and 1972, IRS LISS III images from 1998 to 2008. The analysis suggests an overall bank erosion of 150.04 km^2 and an overall accretion of 61.86 km^2 in Brahmaputra River near Kaziranga National Park, resulting in a loss of 88.188 km^2 area of the park during 1912–2008. In another attempt, Debnath et al. (2017) investigated the bank erosion and channel migration of the Khowai River of Tripura between 1975 and 2014 using Survey of India topographical maps (1:50,000), and Landsat images. The results of the study indicate that the lateral erosion is highly predominant in the Khowai River, where the maximum erosion along the left and right banks was 724.62 m and 533.88 m respectively. Dewan et al. (2017) used multi-temporal Landsat data to analyze channel dynamics of the Ganges-Padma system in Bangladesh from 1973 to 2011. The estimates of the extent of areas of erosion and accretion showed that both the river banks experienced considerable loss of land, i.e., the total net loss for the left bank and the right bank was 155 and 28 km^2, respectively.

The channel morphological studies carried out in the regional context discussed the major driving mechanisms for erosion along the river banks (e.g., Goswami et al., 1999; Jain and Sinha, 2004; Sarma, 2005; Das et al., 2007). The major causative factors for the channel morphological changes are high water discharge and sediment load, the formation of mid-channel bars and obstruction of the flow, changes in the channel slope, sedimentological readjustments, changes in land use and active regional tectonics. The comparison of the rates of bank erosion/deposition in the lower reaches of the Krishna River with the rivers draining the Himalayan region indicates that the river channel reaches of Krishna are relatively stable, probably a result of the flow regulation of the river.

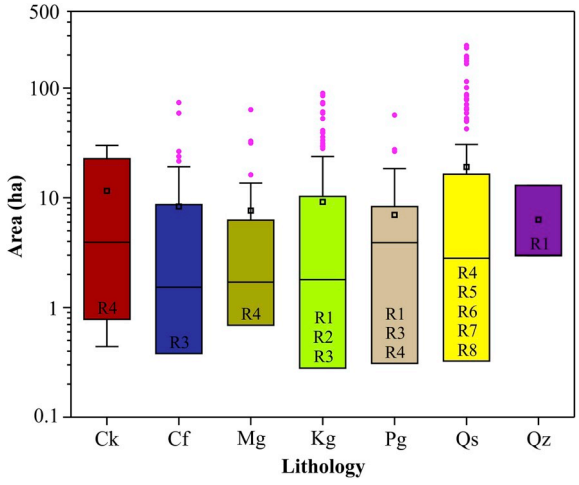

Fig. 13. Variability of bank erosion (1973–2015) in different lithological types (Ck-Charnockite, Cf-Cumbum Formation, Mg-Migmatite Complex, Kg-rocks of Kurnool Group, Pg-Potassic granodiorite to granite, Qs-Quaternary sediments and Qz-Srisailam Quartzite).

6. Summary and conclusion

The present study assessed bank line changes of the lower reaches of the Krishna River that occurred between 1973 and 2015, using multi-temporal Landsat images. The total length of the study reaches is 318 km (i.e., downstream of the Nagarjuna Sagar Dam to the Krishna Delta). The mean width of the river reaches showed significant spatial variability with an irregular downstream trend, which is primarily the result of the topographic and geological controls.

During 1973–1991, the total area of bank erosion was 3093 ha, where 1792 ha was contributed by the left bank, and 1301 ha along the right bank. However, during 1991–2015, the erosion along the banks was reduced to 1386 ha, where erosion was relatively higher along the right bank (830 ha), compared to the left bank (556 ha). The total deposition area along the banks during 1973–199 was 1924 ha, where 527 ha was along the left bank and 1397 ha was along the right bank,

while during 1991–2015, the total area under deposition was increased (2880 ha), where 1600 ha was contributed by the left bank and 1280 ha by the right bank. During 1973–1991, bank erosion was predominant in most of the reaches, compared to bank deposition, whereas the pattern was reversed during 1991–2015. Even though the individual river reaches showed different shifting patterns during the assessment periods, most of the reaches shifted their bank lines without much affecting the bankfull width, i.e., erosion in one bank, while deposition on the other.

Bank erosion of the lower reaches is influenced by floods, and the contrasting nature of bank erosion between 1973-1991 and 1991–2015 can be correlated with the differences in the flood event pattern between the periods. The period, 1973–1991 was characterized by frequently occurring, low magnitude flood events of longer duration, whereas 1991–2015 was considered as infrequent, high magnitude floods of shorter duration. The impact of the Nagarjuna Sagar Dam on bank erosion is apparent as an abrupt increase in the erosion intensity downstream of the dam. The marked variations in bank erosion between the reaches are also strongly linked with the variations in regional lithology, specifically from the rocks of Kurnool Group and Cumbum Formation and peninsular gneisses to Quaternary sediments.

Although the peninsular rivers of India are considered to be stable, compared to the Himalayan Rivers, the dynamic pattern of erosion and deposition along the lower reaches of the Krishna River during 1973–2015 holds further implications for the identification of spatial variations in the process dominance and individual contributions of the process domains.

Declaration of competing interest

The authors hereby declare no conflict of interest with the revised manuscript titled **"Channel stability assessment in the lower reaches of the Krishna River (India) using multi-temporal satellite data during 1973–2015"** (Manuscript ID# RSASE_2019_93).

Acknowledgments

This study was a part of the project funded by the Central Water Commission (Reference No. 4/19/2012/IITM/Morpho/179-191 dated 18-03-2015). The help rendered by Rohith A. N. and Jesna, IIT Madras (for hydrological data analysis), Dr. Vamsi Krishna Vema (Purdue University) and Water Resources Department, Andhra Pradesh State (for facilitating field data collection) are greatly acknowledged. The authors are also thankful to the anonymous reviewers and the editor for their critical and constructive comments.

Appendix A. Supplementary data

Supplementary data to this article can be found online at https://doi.org/10.1016/j.rsase.2019.100274.

References

Abate, M., Nyssen, J., Steenhuis, T.S., Moges, M.M., Tilahun, S.A., Enku, T., Adgo, E., 2015. Morphological changes of Gumara river channel over 50 years, upper Blue Nile basin, Ethiopia. J. Hydrol. 525, 152–164. https://doi.org/10.1016/j.jhydrol.2015.03.044.

Akhtar, M.P., Sharma, N., Ojha, C.S.P., 2011. Braiding process and bank erosion in the Brahmaputra River. Int. J. Sediment Res. 26 (4), 431–444. https://doi.org/10.1016/S1001-6279(12)60003-1.

Amarasinghe, U.A., Sharma, B.R., Aloysius, N., Scott, C., Smakhtin, V., de Fraiture, C., Sinha, A.K., Shukla, A.K., 2005. Spatial Variation of Water Supply and Demand across River Basins of India. Research Report 83. International Water Management Institute, Colombo, Sri Lanka.

APWRDC, 2009. Managing Historic Flood in Krishna River Basin in October 2009. Andhra Pradesh Water Resources Development Corporation, Hyderabad.

ASCE Task Committee on Hydraulics, 1998. Bank mechanics, and modeling of river width adjustment, 1998. River width adjustment, I: processes and mechanisms. J. Hydraul. Eng. 124 (9), 881–902. https://doi.org/10.1061/(ASCE)0733-9429, 124: 9(881).

Biggs, T.W., Gaur, A., Scott, C.A., Thenkabail, P., Parthasaradhi, G.R., Gumma, M.K., Acharya, S., Turral, H., 2007. Closing of the Krishna Basin: irrigation, streamflow depletion and macroscale hydrology. Research Report 111. International Water Management Institute, Colombo, Sri Lanka.

Booth, D.B., Henshaw, P.C., 2001. Rates of channel erosion in small urban streams. In: Wigmosta, M., Burges, S. (Eds.), Land Use and Watersheds: Human Influence on Hydrology and Geomorphology in Urban and Forest Areas. Water Science and Application 2. American Geophysical Union, Washington DC, pp. 17–38.

Brierley, G.J., Fryirs, K.A., Boulton, A., Cullum, C., 2008. Working with change: the importance of evolutionary perspectives in framing the trajectory of river adjustment. In: Brierley, G., Fryirs, K.A. (Eds.), River Futures: an Integrative Scientific Approach to River Repair. Society for Ecological Restoration International. Island Press, Washington DC, pp. 65–84.

Church, M., 2006. Bed material transport and the morphology of alluvial river channels. Annu. Rev. Earth Planet Sci. 34, 325–354. https://doi.org/10.1146/annurev.earth.33.092203.122721.

Coles, S., 2001. An Introduction to Statistical Modelling of Extreme Values. Springer, London.

Comiti, F., Da Canal, M., Surian, N., Mao, L., Picco, L., Lenzi, M.A., 2011. Channel adjustments and vegetation cover dynamics in a large gravel bed river over the last 200 years. Geomorphology 125 (1), 147–159. https://doi.org/10.1016/j.geomorph.2010.09.011.

Couper, P.R., Maddock, I.P., 2001. Subaerial river bank erosion processes and their interaction with other bank erosion mechanisms on the River Arrow, Warwickshire, UK. Earth Surf. Process. Landforms 26 (6), 631–646. https://doi.org/10.1002/esp.212.

Das, B., 2011. Stakeholders' perception in identification of river bank erosion hazard: a case study. Nat. Hazards 58 (3), 905–928. https://doi.org/10.1007/s11069-010-9698-z.

Das, J.D., Dutta, T., Saraf, A.K., 2007. Remote sensing and GIS application in change detection of the Barak river channel, N.E. India. J. Indian Soc. Remote Sens. 35 (4), 301–312.

Debnath, J., Das (Pan), N., Ahmed, I., Bhowmik, M., 2017. Channel migration and its impact on land use/land cover using RS and GIS: a study on Khowai River of Tripura, North-East India. Egypt. J. Remote Sens. Space Sci. 20 (2), 197–201. https://doi.org/10.1016/j.ejrs.2017.01.009.

Dewan, A., Corner, R., Saleem, A., Rahman, M.M., Haider, M.R., Rahman, M.M., Sarker, M.H., 2017. Assessing channel changes of the Ganges-Padma River system in Bangladesh using Landsat and hydrological data. Geomorphology 276, 257–279. https://doi.org/10.1016/j.geomorph.2016.10.017.

Downs, P.W., Dusterhoff, S.R., Sears, W.A., 2013. Reach-scale channel sensitivity to multiple human activities and natural events: lower Santa Clara River, California, USA. Geomorphology 189, 121–134. https://doi.org/10.1016/j.geomorph.2013.01.023.

Florsheim, J.L., Mount, J.F., Chin, A., 2008. Bank erosion as a desirable attribute of rivers. Bioscience 58 (6), 519–529. https://doi.org/10.1641/B580608.

Gamage, N., Smakhtin, V., 2009. Do river deltas in east India retreat? a case study of the Krishna delta. Geomorphology 103 (4), 533–540. https://doi.org/10.1016/j.geomorph.2008.07.022.

Gilvear, D.J., 1999. Fluvial geomorphology and river engineering: future roles utilizing a fluvial hydrosystems framework. Geomorphology 31 (1–4), 229–245. https://doi.org/10.1016/S0169-555X(99)00086-0.

Goswami, U., Sarma, J.N., Patgiri, A.D., 1999. River channel changes of the Subansiri in Assam, India. Geomorphology 30 (3), 227–244. https://doi.org/10.1016/S0169-555X(99)00032-X.

Gregory, K.J., 2006. The human role in changing river channels. Geomorphology 79 (3–4), 172–191. https://doi.org/10.1016/j.geomorph.2006.06.018.

Groombridge, B., Jenkins, M., 1998. Freshwater biodiversity: a preliminary global assessment. World Conservation Monitoring Centre Biodiversity Series No. 8. World Conservation Press, Cambridge.

Gunnell, Y., 1997. Relief and climate in South Asia: the influence of the western Ghats on the current climate pattern of peninsular India. Int. J. Climatol. 17 (11), 1169–1182. https://doi.org/10.1002/(SICI)1097-0088(199709)17:11<1169::AID-JOC189>3.0.CO;2-W.

Gupta, N., Atkinson, P.M., Carling, P.A., 2013. Decadal length changes in the fluvial planform of the river Ganga: bringing a mega-river to life with Landsat archives. Remote Sens. Lett. 4 (1), 1–9. https://doi.org/10.1080/2150704X.2012.682658.

Gurnell, A.M., 1997. Channel change on the River Dee meanders, 1946–1992, from the analysis of air photographs. Regul. Rivers Res. Manag. 13 (1), 13–26. https://doi.org/10.1002/(SICI)1099-1646(199701)13:1<13::AID-RRR420>3.0.CO;2-W.

Hossain, M.A., Gan, T.Y., Baki, A.B.M., 2013. Assessing morphological changes of the Ganges river using satellite images. Quat. Int. 304, 142–155. https://doi.org/10.1016/j.quaint.2013.03.028.

Hupp, C.R., Schenk, E.R., Richter, J.M., Peet, R.K., Townsend, P.A., 2009. Bank erosion along the dam-regulated lower Roanoke River, North Carolina. In: James, L.A., Rathburn, S.L., Whittecar, G.R. (Eds.), Management and Restoration of Fluvial Systems with Broad Historical Changes and Human Impacts, vol 451. Geological Society of America Special Paper, pp. 97–108. https://doi.org/10.1130/2009.2451(06).

Jain, V., Sinha, R., 2004. Fluvial dynamics of an anabranching river system in Himalayan foreland basin, Baghmati river, north Bihar plains, India. Geomorphology 60 (1–2), 147–170. https://doi.org/10.1016/j.geomorph.2003.07.008.

Jain, S.K., Agarwal, P.K., Singh, V.P., 2007. Hydrology and Water Resources of India. Springer, Netherlands.

Jiang, H., Feng, M., Zhu, Y., Lu, N., Huang, J., Xiao, T., 2014. An automated method for extracting rivers and lakes from Landsat imagery. Remote Sens. 6 (6), 5067–5089. https://doi.org/10.3390/rs6065067.
Joshi, S., Jun, X.Y., 2018. Recent changes in channel morphology of a highly engineered alluvial river-the Lower Mississippi River. Phys. Geogr. 39 (2), 140–165. https://doi.org/10.1080/02723646.2017.1340027.
Knighton, D., 1984. Fluvial Forms and Processes. Edward Arnold, London.
Korhonen, J., Kuusisto, E., 2010. Long term changes in the discharge regime in Finland. Nord. Hydrol 41 (3–4), 253–268. https://doi.org/10.2166/nh.2010.112.
Lane, S.N., Tayefi, V., Reid, S.C., Yu, D., Hardy, R.J., 2007. Interactions between sediment delivery, channel change, climate change and flood risk in a temperate upland environment. Earth Surf. Process. Landforms 32 (3), 429–446. https://doi.org/10.1002/esp.1404.
Lawler, D.M., 1993. The measurement of river bank erosion and lateral channel change: a review. Earth Surf. Process. Landforms 18 (9), 777–821. https://doi.org/10.1002/esp.3290180905.
Leopold, L.B., Wolman, M.G., Miller, J.P., 1964. Fluvial Processes in Geomorphology. Dover Publications, New York.
Merritt, D.M., Wohl, E.E., 2003. Downstream hydraulic geometry and channel adjustment during a flood along an ephemeral, arid-region drainage. Geomorphology 52 (3–4), 165–180. https://doi.org/10.1016/S0169-555X(02)00241-6.
Morais, E.S., Rocha, P.C., Hooke, J., 2016. Spatiotemporal variations in channel changes caused by cumulative factors in a meandering river: the lower Peixe River, Brazil. Geomorphology 273, 348–360. https://doi.org/10.1016/j.geomorph.2016.07.026.
MoWR, 2014. WRIS-India Report on Krishna Basin, Version 2.0. Ministry of Water Resources, Government of India.
MoWR, 2016. Annual Report 2015-16. Ministry of Water Resources, Government of India.
Mukherjee, R., Bilas, R., Biswas, S.S., Pal, R., 2017. Bank erosion and accretion dynamics explored by GIS techniques in lower Ramganga river, Western Uttar Pradesh, India. Spatial Info. Res. 25 (1), 23–38. https://doi.org/10.1007/s41324-016-0074-2.
Mutton, D., Haque, C.E., 2004. Human vulnerability, dislocation and resettlement: adaptation processes of river-bank erosion-induced displaces in Bangladesh. Disasters 28 (1), 41–62. https://doi.org/10.1111/j.0361-3666.2004.00242.x.
Nilsson, C., Reidy, C.A., Dynesius, M., Revenga, C., 2005. Fragmentation and flow regulation of the world's large river systems. Science 308 (5720), 405–408. https://doi.org/10.1126/science.1107887.
Ouchi, S., 1985. Response of alluvial rivers to slow active tectonic movement. GSA Bull. 96 (4), 504–515. https://doi.org/10.1130/0016-7606(1985)96<504:ROARTS>2.0.CO;2.
Petts, G.E., 1979. Complex response of river channel morphology subsequent to reservoir construction. Prog. Phys. Geogr. 3 (3), 329–362. https://doi.org/10.1177/030913337900300302.
Petts, G.E., Gurnell, A.M., 2005. Dams and geomorphology: research progress and future directions. Geomorphology 71 (1–2), 27–47. https://doi.org/10.1016/j.geomorph.2004.02.015.
Phillips, J.D., Slattery, M.C., Musselman, Z.A., 2004. Dam-to-delta sediment inputs and storage in the lower Trinity River Texas. Geomorphology 62 (1–2), 17–34. https://doi.org/10.1016/j.geomorph.2004.02.004.
Piegay, H., Cuaz, M., Javelle, E., Mandier, P., 1997. Bank erosion management based on geomorphological, ecological and economic criteria on the Galuare River, France. Regul. Rivers Res. Manag. 13 (5), 433–448. https://doi.org/10.1002/(SICI)1099-1646(199709/10)13:5<433::AID-RRR467>3.0.CO;2-L.
Piegay, H., Darby, S.E., Mosselman, E., Surian, N., 2005. A review of techniques available for delimiting the erodible river corridor: a sustainable approach to managing bank erosion. River Res. Appl. 21, 773–789. https://doi.org/10.1002/rra.881.
Radoane, M., Obreja, F., Cristea, I., Mihaila, D., 2013. Changes in the channel-bed level of the eastern Carpathian rivers: climatic vs. human control over the last 50 years. Geomorphology 193, 91–111. https://doi.org/10.1016/j.geomorph.2013.04.008.
Rao, K.N., Subraelu, P., Naga Kumar, K.ChV., Demudu, G., Hema Malini, B., Rajawat, A. S., Ajai, 2010. Impacts of sediment retention by dams on delta shoreline recession: evidences from the Krishna and Godavari deltas, India. Earth Surf. Process. Landforms 35 (7), 817–827. https://doi.org/10.1002/esp.1977.
Richard, G.A., Julien, P.Y., Baird, D.C., 2005. Statistical analysis of lateral migration of the Rio Grande, New Mexico. Geomorphology 71 (1–2), 139–155. https://doi.org/10.1016/j.geomorph.2004.07.013.
Rinaldi, M., 2003. Recent channel adjustments in alluvial rivers of Tuscany, Central Italy. Earth Surf. Process. Landforms 28 (6), 587–608. https://doi.org/10.1002/esp.464.
Rozo, M.G., Nogueira, A.C.R., Castro, C.S., 2014. Remote sensing-based analysis of the planform changes in the Upper Amazon River over the period 1986-2006. J. South Am. Earth Sci. 51, 28–44. https://doi.org/10.1016/j.jsames.2013.12.004.
Sarkar, A., Garg, R.D., Sharma, N., 2012. RS-GIS based assessment of river dynamics of Brahmaputra River in India. J. Water Resour. Prot. 4 (2), 63–72. https://doi.org/10.4236/jwarp.2012.42008.
Sarma, J.N., Acharjee, S., 2012. A GIS based study on bank erosion by the river Brahmaputra around Kaziranga National Park, Assam, India. Earth Syst. Dyn. Discuss. 3 (2), 1085–1106. https://doi.org/10.5194/esdd-3-1085-2012.
Sarma, J.N., Borah, D., Goswami, U., 2007. Change of river channel and bank erosion of the Burhi Dihing River (Assam), assessed using remote sensing data and GIS. J. Indian Soc. Remote Sens. 35 (1), 93–100. https://doi.org/10.1007/BF02991837.
Sarma, J.N., 2005. Fluvial process and morphology of the Brahmaputra River in Assam, India. Geomorphology 70 (3–4), 226–256. https://doi.org/10.1016/j.geomorph.2005.02.007.
Schumm, S.A., Dumont, J.F., Holbrook, J.M., 2000. Active Tectonics and Alluvial Rivers. Cambridge University Press, New York.
Schumm, S.A., 2005. River Variability and Complexity. Cambridge University Press, New York.
Sharma, N., 1995. Modelling of Braided Alluvial Channels. Ph.D. thesis. University of Roorkee, Roorkee, India.
Sharma, N., 2004. Mathematical modelling and braid indicators. In: Singh, V.P. (Ed.), The Brahmaputra River Basin Water Resources. Kluwer Academic Publishers, Dordrecht, pp. 229–260.
Shields Jr., F.D., Simon, A., Steffen, L.J., 2000. Reservoir effects on downstream river channel migration. Environ. Conserv. 27 (1), 54–66.
Simon, A., Curini, A., Darby, S., Lagendoen, E.J., 1999. Streambank mechanics and the role of bank and near-bank processes in incised channels. In: Darby, S.E., Simon, A. (Eds.), Incised River Channels. John Wiley, Chichester, pp. 123–152.
Simon, A., Curini, A., Darby, S.E., Langendoen, E.J., 2000. Bank and near-bank processes in an incised channel. Geomorphology 35 (3–4), 193–217. https://doi.org/10.1016/S0169-555X(00)00036-2.
Simon, A., Castro, J., Rinaldi, M., 2016. Analysis of processes and forms: water and sediment interactions. In: Kondolf, G.M., Piegay, H. (Eds.), Tools in Fluvial Geomorphology. John Wiley & Sons, Chichester, pp. 237–259.
Smakhtin, V., Anputhas, M., 2009. An assessment of environmental flow requirements of Indian river basins. In: Amarasinghe, U.A., Shah, T., Malik, R.P.S. (Eds.), Strategic Analyses of the National River Linking Project (NRLP) of India, Series 1. India's Water Future: Scenarios and Issues. International Water Management Institute (IWMI), Colombo, Sri Lanka, pp. 293–328.
Sudhakar, K., Sudhakar, M., 2019. Estimation of erosion and deposition of Krishna River bank using remote sensing & GIS. Int. J. Recent Technol. Eng. 7, 888–891.
Surian, N., 1999. Channel changes due to river regulation: the case of the Piave River, Italy. Earth Surf. Process. Landforms 24 (12), 1135–1151. https://doi.org/10.1002/(SICI)1096-9837(199911)24:12<1135::AID-ESP40>3.0.CO;2-F.
Surian, N., Rinaldi, M., 2003. Morphological response to river engineering and management in alluvial channels in Italy. Geomorphology 50 (4), 307–326. https://doi.org/10.1016/S0169-555X(02)00219-2.
Ta, W., Jia, X., Wang, H., 2013. Channel deposition induced by bank erosion in response to decreased flows in the sand-banked reach of the upstream Yellow River. Catena 105, 62–68. https://doi.org/10.1016/j.catena.2013.01.007.
Takagi, T., Oguchi, T., Matsumoto, J., Grossman, M.J., Sarker, M.H., Matin, M.A., 2007. Channel braiding and stability of the Brahmaputra River, Bangladesh, since 1967: GIS and remote sensing analyses. Geomorphology 85 (3–4), 294–305. https://doi.org/10.1016/j.geomorph.2006.03.028.
Thorne, C.R., 1982. Processes and mechanisms of river bank erosion. In: Hey, R.D., Bathurst, J.C., Thorne, C.R. (Eds.), Gravel-Bed Rivers. Wiley, Chichester, pp. 227–271.
Thorne, C.R., Russell, P.G., Alam, M.K., 1993. Planform pattern and channel evolution of the Brahmaputra River, Bangladesh. In: Best, J.L., Bristow, C.S. (Eds.), Braided Rivers. Geological Society of London Special Publication, vol 75. Geological Society, London, pp. 257–276.
Tiegs, S.D., Pohl, M., 2005. Planform channel dynamics of the lower Colorado River: 1976-2000. Geomorphology 69 (1–4), 14–27. https://doi.org/10.1016/j.geomorph.2004.12.002.
Tooth, S., McCarthy, T.S., Brandt, D., Hancox, P.J., Morris, R., 2002. Geological controls on the formation of alluvial meanders and floodplain wetlands: the example of the Klip River, eastern Free State, South Africa. Earth Surf. Process. Landforms 27 (8), 797–815. https://doi.org/10.1002/esp.353.
Venot, J.P., 2009. Rural dynamics and new challenges in the Indian water sector: trajectory of the Krishna Basin South India. In: Molle, F., Wester, P. (Eds.), River Basins Trajectories: Societies, Environments and Development. International Water Management Institute, Colombo, Sri Lanka & CABI Publishing, Wallingford, pp. 214–237. https://doi.org/10.1079/9781845935382.0214.
Venot, J.P., Bharati, L., Giordano, M., Molle, F., 2011. Beyond water, beyond boundaries: spaces of water management in the Krishna river basin, South India. Geogr. J. 177 (2), 160–170. https://doi.org/10.1111/j.1475-4959.2010.00384.x.
Winterbottom, S.J., 2000. Medium and short-term channel planform changes of the rivers Tay and Tummel, Scotland. Geomorphology 34 (3–4), 195–208. https://doi.org/10.1016/S0169-555X(00)00007-6.
Yang, X., Damen, M.C.J., van Zuidam, R.A., 1999. Satellite remote sensing and GIS for the analysis of channel migration changes in the active Yellow River Delta, China. Int. J. Appl. Earth Obs. Geoinf. 1 (2), 146–157. https://doi.org/10.1016/S0303-2434(99)85007-7.
Yang, S.L., Zhang, J., Xu, X.J., 2007. Influence of the three Gorges dam on downstream delivery of sediment and its environmental implications, Yangtze river. Geophys. Res. Lett. 34 (10), L10401. https://doi.org/10.1029/2007GL029472.
Yao, Z., Ta, W., Jia, X., Xiao, J., 2011. bank erosion and accretion along the Ningxia-inner Mongolia reaches of the Yellow River from 1958 to 2008. Geomorphology 127 (1–2), 99–106. https://doi.org/10.1016/j.geomorph.2010.12.010.
Zhang, W., Yuan, J., Han, J., Huang, C., Li, M., 2016. Impact of the three Gorges dam on sediment deposition and erosion in the middle Yangtze river: a case study of the Shashi reach. Nord. Hydrol 47 (S1), 175–186. https://doi.org/10.2166/nh.2016.092.